Nanobubble Assembly

International Edition: DOI: 10.1002/anie.201505817
German Edition: DOI: 10.1002/ange.201505817

Stable Encapsulated Air Nanobubbles in Water

Yu Wang, Guojun Liu, Heng Hu, Terry Yantian Li, Amer M. Johri, Xiaoyu Li, and Jian Wang*

Abstract: *The dispersion into water of nanocapsules bearing a highly hydrophobic fluorinated internal lining yielded encapsulated air nanobubbles. These bubbles, like their micrometer-sized counterparts (microbubbles), effectively reflected ultrasound. More importantly, the nanobubbles survived under ultrasonication 100-times longer than a commercial microbubble sample that is currently in clinical use. We justify this unprecedented stability theoretically. These nanobubbles, owing to their small size and potential ability to permeate the capillary networks of tissues, may expand the applications of microbubbles in diagnostic ultrasonography and find new applications in ultrasound-regulated drug delivery.*

Trapping air in the central cavity of solid nanocapsules yields encapsulated air bubbles. If these bubbles are stable and reflect and scatter ultrasound effectively (being echogenic), they will expand the applications of micrometer-sized bubbles (microbubbles) that are currently used as contrast agents in diagnostic ultrasonography.[1–4] For example, they may find applications in the diagnosis of tumors, or in the imaging of blood perfusion owing to the ability of nanobubbles to permeate the capillary networks of organs.[5–7] Furthermore, nanobubbles bearing surface recognition functionalities may be useful in ultrasound-regulated drug delivery because their pathways can be visualized by ultrasonography and their carried drugs can be released at the targeted sites by more powerful pulses.[5,8] However, stable air nanobubbles in water are difficult to prepare.[9] In fact, even the term "nanobubbles" is currently misused to refer to nanoemulsion droplets of fluorinated liquids that readily gasify under ultrasonication to generate transient bubbles.[5,6] Herein, we report the stabilization of air bubbles in nanocapsules bearing a highly hydrophobic fluorinated internal lining. These nanobubbles reflected ultrasound effectively. More importantly, the nanobubbles withstood ultrasonication approximately 100-times longer than a third-generation microbubble sample. The latter bubbles are among the most stable commercial bubbles and are much more stable than the first-generation naked air microbubbles and the second-generation encapsulated air microbubbles, because their filling gas (perfluorinated propane) is much less soluble in water than air.[1]

Air nanobubbles are unstable in water because they possess a large surface area-to-volume ratio and are energetically costly to create. Furthermore, a spherical nanobubble of radius r has an internal Laplace pressure P_L of $2\gamma_w/r$,[10] where the surface tension of water γ_w is 72.1 mN m^{-1} at room temperature.[11] At $r = 50$ nm, P_L is 29.4 atm and this value increases as r decreases. Thus, air-filled nanobubbles readily dissipate when they are perturbed by ultrasound, for example.[1] Air bubbles dissipate, even without mechanical disturbance, by air solubilization once water becomes unsaturated owing to atmospheric pressure changes.[9,12,13] Nanobubbles dissipate faster than microbubbles in unsaturated water because of their higher internal Laplace pressure and thus higher air solubility at the bubble and water interface.[14]

Encapsulation slows down air diffusion from an encapsulated cavity into water and inhibits bubble dissipation.[2,12,14,15] Further, Epstein and Plesset[12] predicted theoretically that bubbles could be stabilized by using an encapsulating material possessing a surface tension of zero.[15] Since such a material has not been discovered,[16,17] there have been no reported efforts on the use of low surface tension materials to encapsulate air bubbles. Rather, the materials used in the past have included phospholipids,[15] polyesters,[18] and polycyanoacrylate.[2] Since the hydrophobic parts of these reagents had surface tensions > 30 mN m^{-1}, they could not effectively stabilize air nanobubbles.

We tried, against conventional thinking, to use fluorinated polymers that have surface tensions as low as 6.7 mN m^{-1} [16] to encapsulate air bubbles because of our prior experience in highly water- and oil-repellant coatings.[19] Water does not enter the spaces between the threads and fibers of an immersed cotton fabric coated by a perfluorinated polymer.[19–21] Instead, a plastron or air layer is trapped between the fabric and water.[19] This trapped plastron layer has also been used to lower the density of fluorinated particles and to float them in water.[22] These phenomena should be analogous to water rejection by a submerged hydrophobic capillary tube that required an external pressure p_B to force water into it:

$$p_B = -\frac{2\gamma_w \cos\theta}{r_c} \quad (1)$$

where θ is the contact angle of water on the internal wall of the capillary and r_c is the radius of the capillary. According to Equation (1), $p_B = 735$ atm at $r_c = 1$ nm and $\theta \approx 120°$, which is the water contact angle on a perfluorinated polymer.[16,23] Therefore, we imagined that a tremendous pressure was required to force water into a fluorinated capsule that might

[*] Y. Wang, G. Liu, H. Hu, X. Li, J. Wang
Department of Chemistry, Queen's University
90 Bader Lane, Kingston, Ontario, K7L 3N6 (Canada)
E-mail: gliu@chem.queensu.ca
T. Y. Li
Department of Biomedical and Molecular Sciences, Queen's University
18 Stuart Street, Kingston, Ontario, K7L 3N6 (Canada)
A. M. Johri
Department of Medicine, Queen's University
Kingston General Hospital FAPC 3, 76 Stuart Street, Kingston, Ontario, K7L 2V7 (Canada)

Supporting information for this article is available on the WWW under http://dx.doi.org/10.1002/anie.201505817.

bear molecular defects with sizes smaller than 1 nm.[16] Consequently, air nanobubbles in fluorinated capsules should be stable even if the surface tension of the capsular lining was not zero.

To verify our hypothesis, we prepared water-dispersible nanocapsules with a fluorinated internal lining from the triblock terpolymer ACF,[24] where A, C, and F denote poly(acrylic acid), poly(2-cinnamoyloxyethyl methacrylate), and poly(2-perfluorooctylethyl methacrylate), respectively (Figure 1 a). Here the A and C blocks were respectively

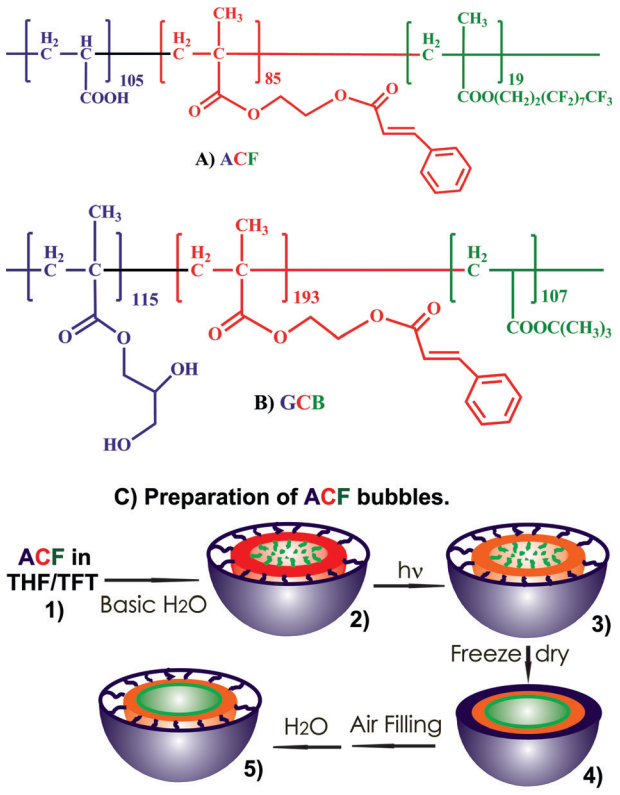

Figure 1. Chemical structures of A) ACF and B) GCB. C) Schematic diagram of the ACF nanobubble preparation process.

chosen for their solubility in water and ability to photocrosslink. For comparison, we also prepared nanocapsules from the triblock terpolymer GCB,[25] where B denotes poly(*tert*-butyl acrylate) and G denotes the water-soluble poly(glyceryl monomethacrylate) block (Figure 1 b). In contrast to F that has a surface tension of 7.5 mN m^{-1} [17] and a water contact angle of 120°,[17,23] B has values corresponding to 30.4 of mN m^{-1} [26] and 75°,[27] respectively. The ACF and GCB samples were well-defined and possessed polydispersity indices less than 1.04 because they were derived from precursors synthesized by anionic polymerization (Supporting Information).

To prepare the ACF nanocapsules, 15.0 mg of ACF was dissolved into tetrahydrofuran (THF, 0.70 mL) before trifluorotoluene (TFT, 1.50 mL) was slowly added. Since the mixture solubilized the C and F blocks but not the A block, the copolymer formed micelles with a hydrodynamic diameter of 96 nm as determined by dynamic light scattering (DLS). We then pumped 8.0 mL of an aqueous 5.0×10^{-3} M NaOH solution over a period of 1 h into this mixture, which was thermostated to 20 °C and stirred at 1800 rpm. We speculate that added water caused the initial micelles to transition to water-swollen micelles, and then to a water-in-oil emulsion stabilized by ACF, and eventually to an oil-in-water emulsion upon phase inversion.[25,28,29] In the final state, the core was probably mainly filled with TFT owing to the solubility of THF in water. Consequently, the internal and external surfaces of the insoluble C wall should be lined by the F and poly(sodium acrylate) chains, respectively (Structure 2, Figure 1 C). Photolysis of these droplets with UV light crosslinked the C walls to yield stable capsules.[30] We then removed TFT and water from the system by freeze drying to yield hollow capsules (Structure 4, Figure 1 C). After backfilling the capsular cavities with air, we stirred the powdery sample in water to disperse encapsulated air nanobubbles. The GCB bubbles were prepared similarly except the NaOH solution was replaced with deionized water during the emulsification step.

The nanocapsules and nanobubbles thus prepared were characterized by DLS, transmission electron microscopy (TEM), and atomic force microscopy (AFM). Figure 2

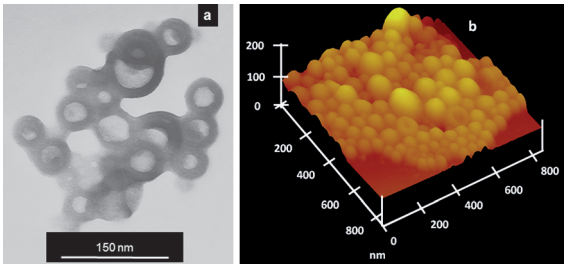

Figure 2. a) TEM and (b) AFM height images of the ACF nanocapsules that had been sprayed onto a cellulose-coated copper grid and a silicon wafer, respectively. The dried TEM specimen was stained with OsO_4.

shows a TEM and an AFM height image of the ACF nanocapsules after they had been sprayed and dried on a cellulose-coated TEM grid and on a silicon wafer, respectively. The observation of the dark rings with a gray center by TEM,[31] and of collapsed bowls by AFM,[25] as well as the large diameter of the particles relative to the length of the fully stretched ACF chains support the targeted capsular structure (Figure 2).[32] At higher magnifications, white dots and stripes were also seen in the TEM images of the capsules. These fine structures should be due to the uneven distribution of the poly(sodium acrylate) chains on the capsular surfaces because similar structures were observed for ACF cylindrical micelles after their surface A chains were stained by uranyl acetate.[24] Successful capsule and nanobubble preparation was also confirmed by data shown in Table S2 (Supporting Information). While the AFM and DLS diameters of the ACF nanobubbles were 115 ± 66 and 204 ± 4 nm, these values increased to 225 ± 73 and 459 ± 10 nm, respectively, for the GCB nanobubbles. Thus, the GCB bubbles were larger and would have a lower Laplace pressure than the ACF bubbles.

As far as P_L was concerned, the GCB bubbles were more stable than the ACF nanobubbles.

We used ultrasonography to detect bubbles and to establish their stability. For such experiments, a vascular ultrasonography device was used in the harmonic mode by sending pulses at 4 MHz and detecting reflected signals at 8 MHz. The artificial vessel consisted of a rubber tube of an inner diameter of 1.0 cm and length of 6.5 cm. This tube was filled with water or human blood and placed in artificial tissue composed of a gelled cellulose matrix (Supporting Information). We began recording two-dimensional (2D) cross-sectional images or videos of the tube along the long axis direction 1 s after a sample in 0.40 mL of water was injected into the tube, and the recorded images were then analyzed to determine their gray-scale brightness readings.

We analyzed in water a total of seven samples, which included an ACF nanoemulsion sample (Structure 3, Figure 1 C), ACF and GCB nanobubble samples that were freshly dispersed into water, ACF and GCB nanobubble samples that were left standing at 21 °C for 4 h, an ACF sample that stood still in water for 3 weeks, and a fresh commercial microbubble sample that consisted of perfluoropropane gas encapsulated in phospholipids. While the first six samples all had a final polymer concentration of 0.125 mg mL^{-1} after their injection into the rubber tube, the concentration of the last sample was unknown but was adjusted so that a reasonable ultrasound signal was obtained.

Our analysis yielded the initial image brightness values of 0.013 (ACF emulsion), 0.372 (fresh ACF bubbles), 0.366 (ACF bubbles aged for 4 h.), 0.379 (ACF bubbles aged for 3 weeks), 0.260 (fresh GCB bubbles), 0.019 (GCB bubbles aged for 4 h), and 0.435 (commercial bubbles). The lack of a significant signal from the ACF nanoemulsion confirmed that neither the polymer nor the encapsulated TFT droplets reflected ultrasound effectively. However, fresh ACF or GCB nanobubbles, just like the commercial microbubbles, readily reflected ultrasound and were echogenic owing to the air trapped in their capsular cavities.

Interestingly, the GCB bubbles lost their signal and became echolucent 4 h after their dispersion in water, suggesting that water seeped through the GCB capsular walls and replaced the air in the cavities. Thus, the B-encapsulated nanobubbles were thermodynamically unstable in water. In contrast, the ACF bubbles 4 h and 3 weeks after their dispersion in water had the same echogenicity as the fresh ones, suggesting that these bubbles were thermodynamically stable.

Strikingly, both the fresh and aged ACF bubbles exhibited better stability than the commercial bubbles under continuous ultrasonication. Figure 3 a compares the 2-D ultrasound images taken at different ultrasonication times after the tube of water was doped with fresh ACF nanobubbles and the commercial microbubbles. The latter sample lost most of its signal after 15 s of ultrasonication. In contrast, the sample containing the ACF nanobubbles became dark only at the top near the ultrasound probe while the bottom section remained bright even after 180 s of ultrasonication. Figure 3 b and c plot the variation in the gray scale values of five samples as a function of the ultrasonication time. The samples that were

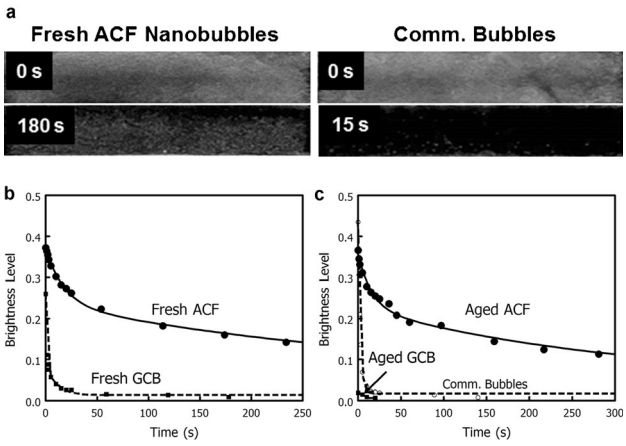

Figure 3. a) 2-D ultrasound images of a tube of water at different times after the injection of the fresh ACF nanobubbles and commercial microbubbles. b and c) Decay in the brightness of ultrasound images of the water-filled tube as a function of the time after the injection of different contrast agents.

doped with fresh ACF nanobubbles and ACF nanobubbles that were aged for 4 h behaved analogously and exhibited long-term stability under ultrasonication. The extraordinary stability was also demonstrated for the ACF nanobubbles that were aged for 3 weeks (Supporting Information). In contrast, the signals of the other samples quickly faded. Therefore, only the F-encapsulated air nanobubbles were exceptionally stable in water.

We fitted the ultrasound signal decay data $I(t)$ of Figure 3 b and c using the following phenomenological equation:

$$I(t) = a_0 + a_1 e^{-t/\tau_1} + a_2 e^{-t/\tau_2} \quad (2)$$

where a_1 and a_2 are the weighting factors for the decay terms with lifetimes τ_1 and τ_2, respectively. The parameters (Supporting Information, Table S3) thus obtained were then used to calculate the average lifetimes for the decaying terms using:

$$\langle\tau\rangle = \frac{a_1\tau_1 + a_2\tau_2}{a_1 + a_2} \quad (3)$$

The average lifetimes thus obtained for the fresh GCB bubbles, the commercial microbubbles, the fresh ACF bubbles, and the aged ACF bubbles were 3.7, 2.5, 226, and 186 s, respectively. While the fresh and aged ACF bubbles had essentially the same longevity, the commercial bubbles and fresh CGB bubbles were equally short-lived. Quantitatively, the lifetime of the ACF bubbles was about 100-times longer than that of the commercial bubbles.

We further compared the behavior of the ACF nanobubbles and the commercial microbubbles in human blood. As in water, the ACF nanobubbles in blood exhibited a greatly improved stability under ultrasonication compared to the commercial microbubbles (Supporting Information).

We analyzed by TEM an ACF capsular sample after 30 min ultrasonication in water and concluded that most of the capsules retained their structural integrity after ultrasoni-

cation (Supporting Information, Figure S1). Therefore, displacement of air by water in the cavities was the main cause for the loss in echogenicity.

To assess the Gibbs free energy change accompanying air displacement by water in the cavities, we consider dilute capsular dispersions in which the capsules are non-interacting, independent, and equivalent. Thus, we focus our analysis on one capsule that is dispersed in a large body of aerated water at constant atmospheric pressure and room temperature. In the initial state, no water is in the capsular cavity with a radius R. However, the cavity is fully filled with water in the final state. From the initial to the final state, the original interface between air and the cavity wall is lost, and a new interface between the wall and water is created. Therefore, the Gibbs free energy change accompanying this process is

$$\Delta G = 4\pi R^2\gamma_{wp} - 4\pi R^2\gamma_p \quad (4)$$

where γ_p is the surface tension of the wall and γ_{wp} is the interfacial tension between the wall and water. According to Young's relation, $\gamma_{wp}-\gamma_p = -\gamma_w\cos\theta$, where θ is the static contact angle of a water droplet on the polymer wall. Thus, Equation (4) simplifies to

$$\frac{\Delta G(R)}{4\pi R^2} = -\gamma_w\cos\theta \quad (5)$$

When the wall material has $\theta = 75°$, the value for B, the free energy change from the initial to the final state is negative. Thus, water spontaneously entered the cavities of the GCB capsules, as observed experimentally. On the other hand, $\Delta G(R)/(4\pi R^2)$ is positive if F made up the cavity wall. Thus, the ACF nanobubbles were thermodynamically stable in water.

In conclusion, we have prepared encapsulated air nanobubbles in water. These bubbles were echogenic and were much more stable under ultrasonication in both water and human blood than a commercial third-generation ultrasonography contrast agent. Results of this work suggest that changing the encapsulating material is a viable approach for the preparation of stable encapsulated air microbubbles and nanobubbles. Owing to the ability for the small nanobubbles to permeate capillary networks of organs and tissues, future versions of these nanobubbles, which may be called fourth-generation bubbles, may find applications in advanced diagnostics and drug delivery.

Acknowledgements

NSERC of Canada is gratefully acknowledged for sponsoring this research. G.L. thanks the Canada Research Chairs Program for a chair position in Materials Science. Prof. Gang Wu is thanked for constructive suggestions on improving our presentation.

Keywords: assembly · block copolymers · nanobubbles · nanocapsules · ultrasonography

How to cite: *Angew. Chem. Int. Ed.* **2015**, *54*, 14291 – 14294
Angew. Chem. **2015**, *127*, 14499 – 14502

[1] H. Becher, P. Burns, *Handbook of Contrast Echocardiography—Left Ventricular Function and Myocardial Perfusion*, Springer, Frankfurt, **2000**.
[2] E. Stride, M. Edirisinghe, *Soft Matter* **2008**, *4*, 2350 – 2359.
[3] K. Ferrara, R. Pollard, M. Borden, *Annu. Rev. Biomed. Eng.* **2007**, *9*, 415 – 447.
[4] M. Postema, G. Schmitz, *Ultrason. Sonochem.* **2007**, *14*, 438 – 444.
[5] R. Cavalli, A. Bisazza, D. Lembo, *Int. J. Pharm.* **2013**, *456*, 437 – 445.
[6] N. Rapoport, K. H. Nam, R. Gupta, Z. G. Gao, P. Mohan, A. Payne, N. Todd, X. Liu, T. Kim, J. Shea, C. Scaife, D. L. Parker, E. K. Jeong, A. M. Kennedy, *J. Controlled Release* **2011**, *153*, 4 – 15.
[7] X. Z. Fan, L. F. Wang, Y. L. Guo, H. P. Tong, L. Li, J. Ding, H. Y. Huang, *Nanotechnology* **2013**, *24*, 325102.
[8] R. Suzuki, T. Takizawa, Y. Negishi, N. Utoguchi, K. Maruyama, *Int. J. Pharm.* **2008**, *354*, 49 – 55.
[9] J. I. Park, E. Tumarkin, E. Kumacheva, *Macromol. Rapid Commun.* **2010**, *31*, 222 – 227.
[10] P. Atkins, *Physical Chemistry*, 6th ed, Freeman, New York, **1998**.
[11] D. R. Lide, *CRC Handbook of Chemistry and Physics*, 76th ed, CRC, Boca Raton, **1995**.
[12] P. S. Epstein, M. S. Plesset, *J. Chem. Phys.* **1950**, *18*, 1505 – 1509.
[13] X. H. Zhang, A. Khan, W. A. Ducker, *Phys. Rev. Lett.* **2007**, *98*, 0.
[14] S. Ljunggren, J. C. Eriksson, *Colloids Surf. A* **1997**, *129*, 151 – 155.
[15] J. J. Kwan, M. A. Borden, *Adv. Colloid Interface Sci.* **2012**, *183*, 82 – 99.
[16] T. Nishino, M. Meguro, K. Nakamae, M. Matsushita, Y. Ueda, *Langmuir* **1999**, *15*, 4321 – 4323.
[17] A. Hirao, K. Sugiyama, H. Yokoyama, *Prog. Polym. Sci.* **2007**, *32*, 1393 – 1438.
[18] W. J. Cui, J. Z. Bei, S. G. Wang, G. Zhi, Y. Y. Zhao, X. S. Zhou, H. W. Zhang, Y. Xu, *J. Biomed. Mater. Res. B* **2005**, *73*, 171 – 178.
[19] D. Xiong, G. Liu, E. J. S. Duncan, *Langmuir* **2012**, *28*, 6911 – 6918.
[20] J. P. Zhang, S. Seeger, *Angew. Chem. Int. Ed.* **2011**, *50*, 6652 – 6656; *Angew. Chem.* **2011**, *123*, 6782 – 6786.
[21] A. Solga, Z. Cerman, B. F. Striffler, M. Spaeth, W. Barthlott, *Bioinspiration Biomimetics* **2007**, *2*, S126 – S134.
[22] J. H. Bahng, B. Yeom, Y. C. Wang, S. O. Tung, J. D. Hoff, N. Kotov, *Nature* **2015**, *517*, 596 – 599.
[23] D. Macoretta, M. Rabnawaz, C. M. Grozea, G. J. Liu, Y. Wang, A. Crumblehulme, M. Wyer, *ACS Appl. Mater. Interfaces* **2014**, *6*, 21435 – 21445.
[24] Y. Gao, X. Y. Li, L. Z. Hong, G. J. Liu, *Macromolecules* **2012**, *45*, 1321 – 1330.
[25] R. H. Zheng, G. J. Liu, *Macromolecules* **2007**, *40*, 5116 – 5121.
[26] F. Pan, P. Wang, K. Lee, A. Wu, N. J. Turro, J. T. Koberstein, *Langmuir* **2005**, *21*, 3605 – 3612.
[27] C. Mengel, A. R. Esker, W. H. Meyer, G. Wegner, *Langmuir* **2002**, *18*, 6365 – 6372.
[28] P. Fernandez, V. Andre, J. Rieger, A. Kuhnle, *Colloids Surf. A* **2004**, *251*, 53 – 58.
[29] N. Anton, J.-P. Benoit, P. Saulnier, *J. Controlled Release* **2008**, *128*, 185 – 199.
[30] A. Guo, G. Liu, J. Tao, *Macromolecules* **1996**, *29*, 2487 – 2493.
[31] L. F. Zhang, A. Eisenberg, *Science* **1995**, *268*, 1728 – 1731.
[32] D. E. Discher, A. Eisenberg, *Science* **2002**, *297*, 967 – 973.

Received: June 24, 2015
Revised: September 11, 2015
Published online: October 6, 2015

